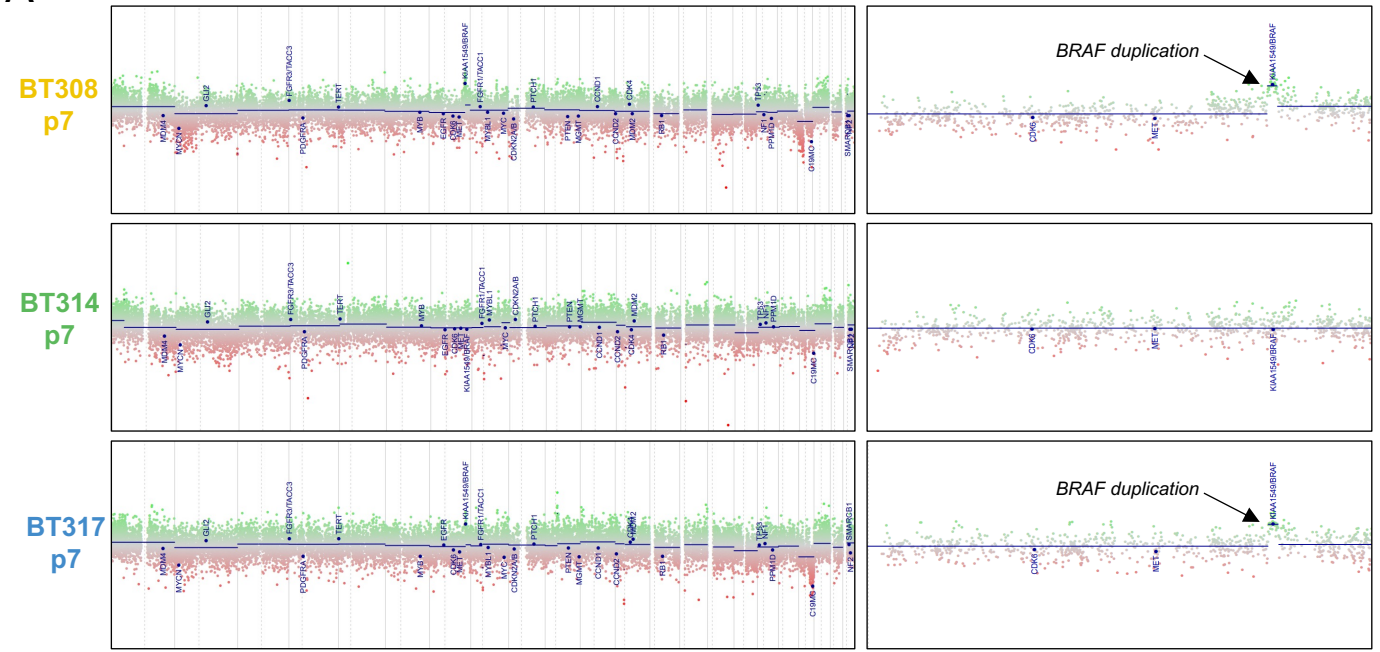


# Supplementary Figure 1

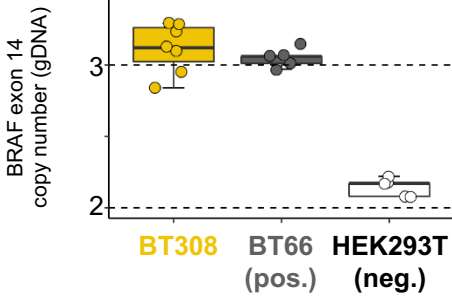
**A**

chromosome 1-22

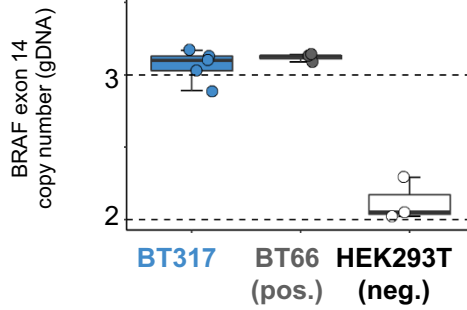
chromosome 7q



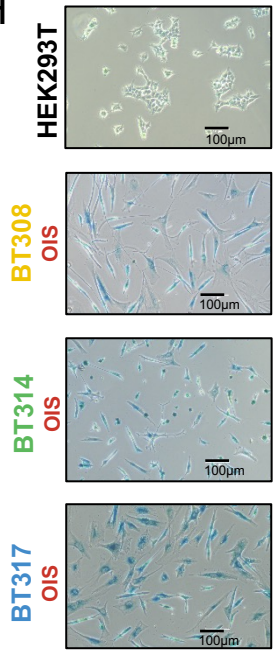
**B**



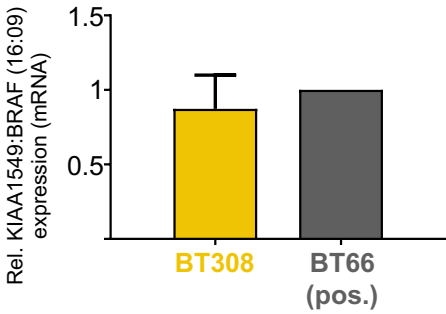
**C**



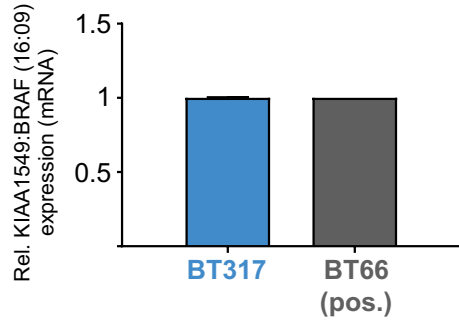
**H**



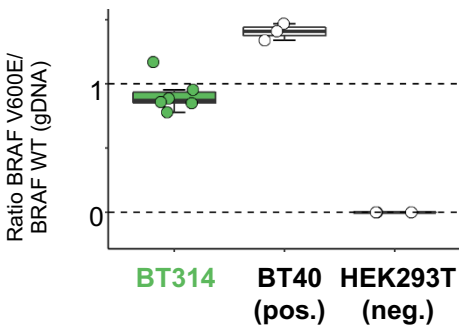
**D**



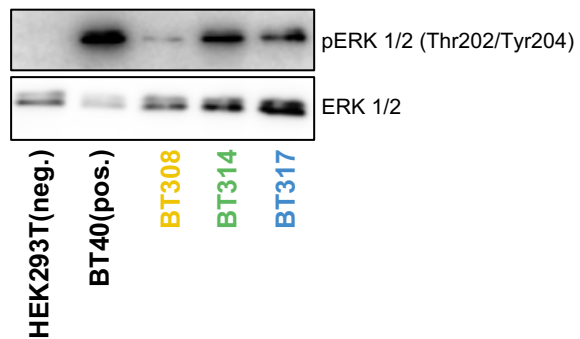
**E**



**F**



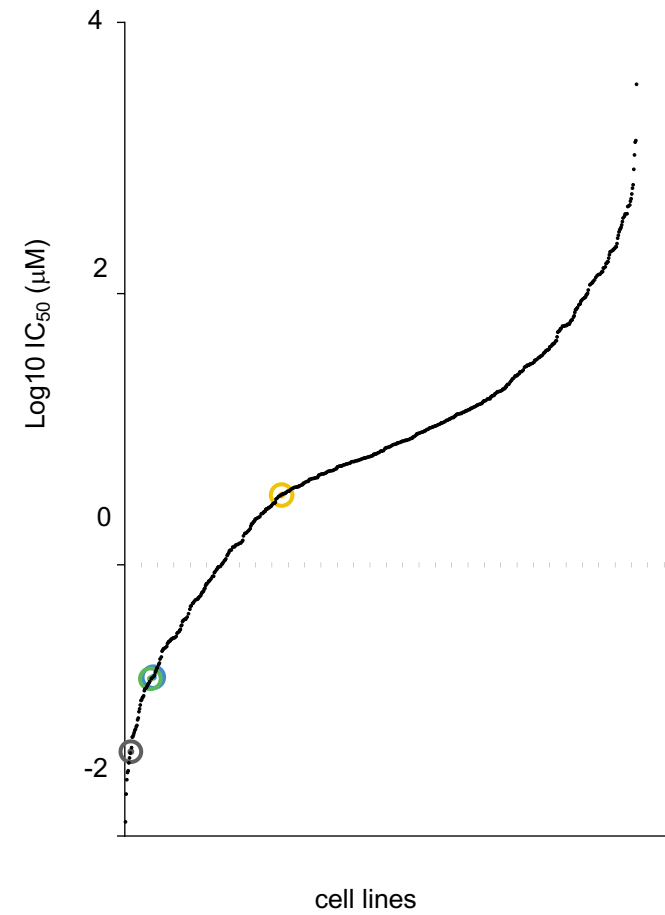
**G**



**Supplementary Figure 1: Characterization of new patient-derived PA *in vitro* models DKFZ-BT308 (BT308), DKFZ-BT314 (BT314) and DKFZ-BT317 (BT317).** **A** DNA methylation derived copy number plots of PA cell lines in proliferation mode at passage 7. Enlarged depiction of chromosome 7q highlights a focal gain indicating the presence of a BRAF duplication. **B, C** Copy number of BRAF exon 14 measured by ddPCR on genomic DNA level (at least n=3 biological replicates) indicating the presence of a BRAF duplication in BT308 and BT317 cells, respectively. DKFZ-BT66 served as positive control (BRAF duplicated) and HEK293T cells were used as BRAF WT control. **D, E** RTqPCR with specific primers detecting the expression of a KIAA1549 (exon 16): BRAF (exon 9) fusion in BT308 (n=3; mean +/-SD) and BT317 (n=3; mean +/- SD), respectively. DKFZ-BT66 served as reference. **F** Ratio of BRAF-V600E/BRAF WT on genomic DNA level (at least n=3 biological replicates) measured by ddPCR mutation assay detecting a BRAF V600E mutation in BT314 cells. A ratio close to 1 indicated a high tumor cell purity. BT40 cells served as positive control (5 copies of BRAF-V600E/cell). **G** Western blot of pERK/ERK expression in 3 PA models compared to MAPK negative control (HEK293T) and MAPK positive control (BT40) **H** Staining for SA- $\beta$ -galactosidase in three PA cell lines in OIS mode (5 days after doxycycline withdrawal, representative pictures). HEK293T cells served as negative control.

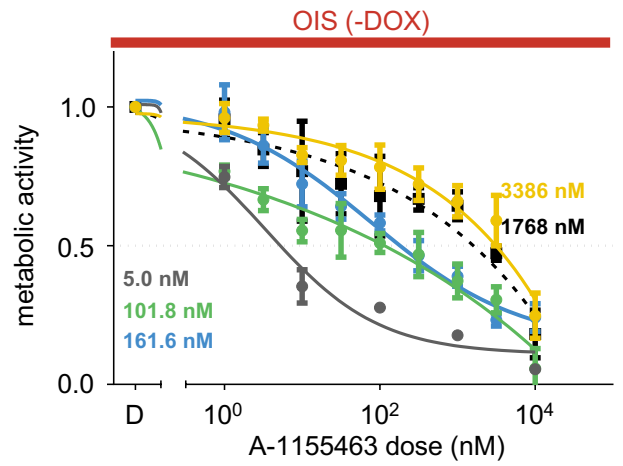
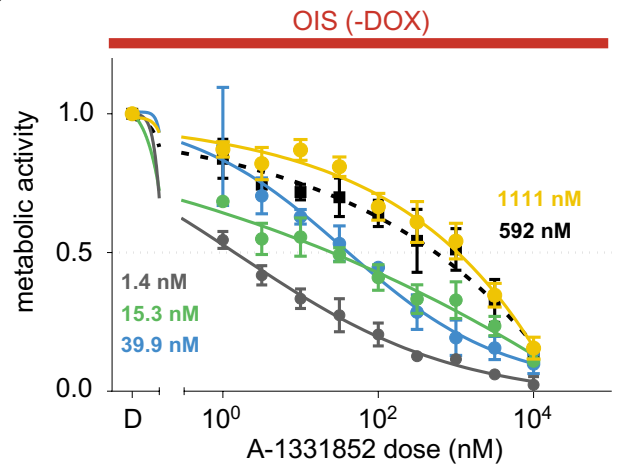
# Supplementary Figure 2

## A



- 751 GDSC cell lines
- ⊙ BT66 OIS (rank 10/755)
- ⊙ BT314 OIS (rank 39/755)
- ⊙ BT317 OIS (rank 43/755)
- ⊙ BT308 OIS (rank 232/755)

## B

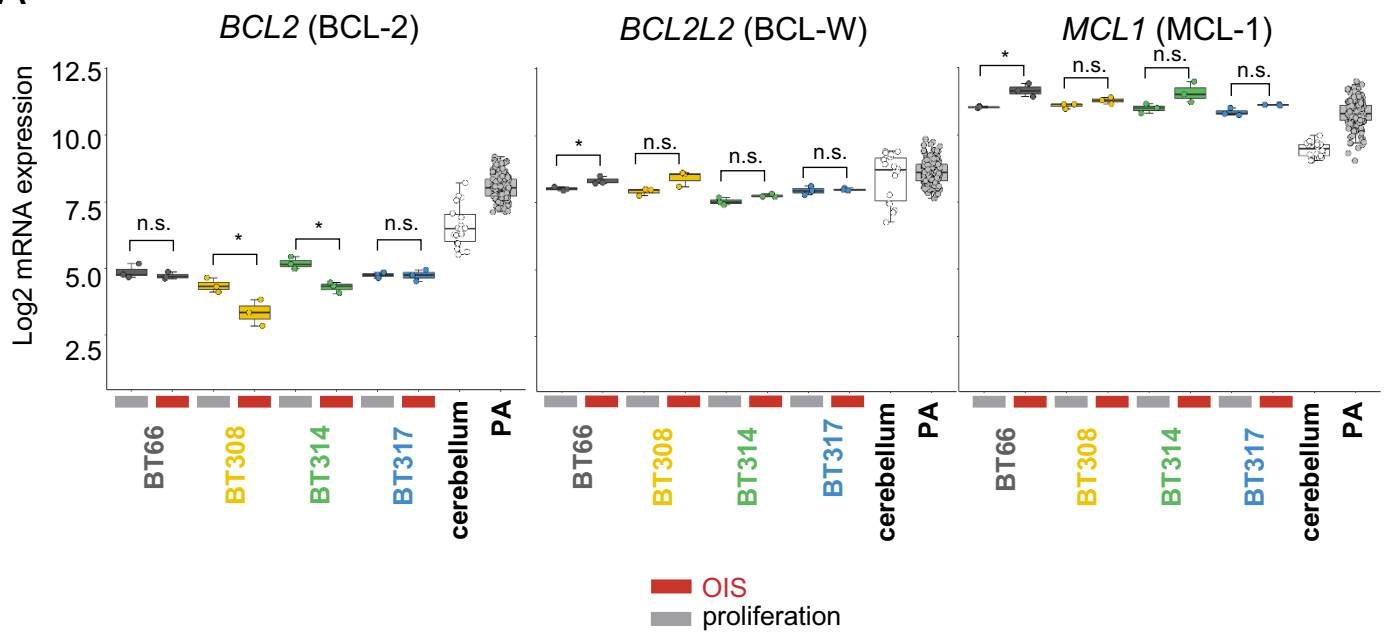


- BT66
- BT308
- BT314
- BT317
- NHA TA<sub>g</sub>
- D DMSO

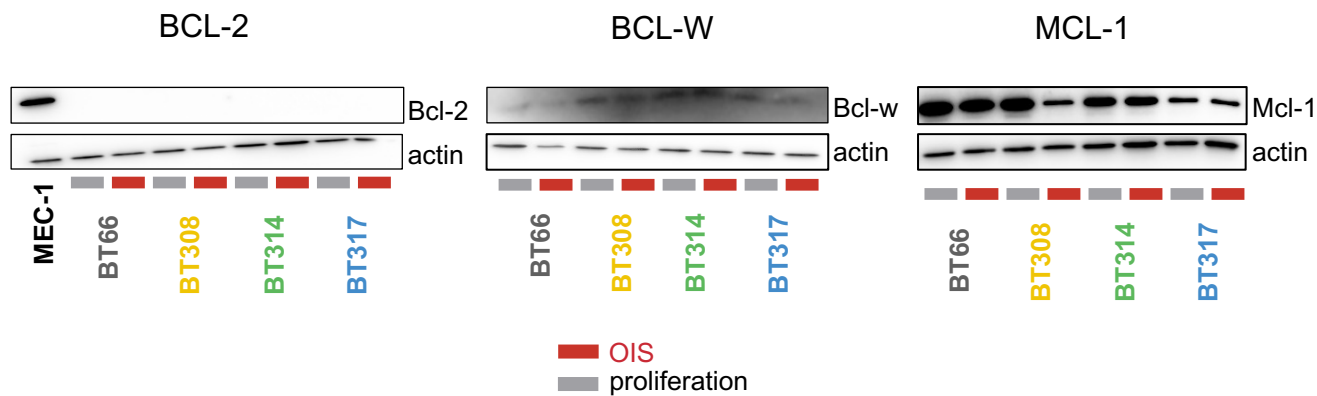
**Supplementary Figure 2: Impact of BH3 mimetics on the metabolic activity of PA cell lines DKFZ-BT66 (BT66), DKFZ-BT308 (BT308), DKFZ-BT314 (BT314) and DKFZ-BT317 (BT317).** **A** ranking of  $IC_{50}$  values of navitoclax in 751 cell lines from GDSC database (GDSC2) and the four PA models in OIS mode. **B** Dose-response curve of A-1331852 and A-1155463, respectively, in four PA cell lines in OIS and normal human astrocytes NHA TA<sub>g</sub> (5 days doxycycline withdrawal). Depicted are means  $\pm$  SD of at least  $n=3$  biological replicates. Absolute  $IC_{50}$  values are given in nM for each cell line.

# Supplementary Figure 3

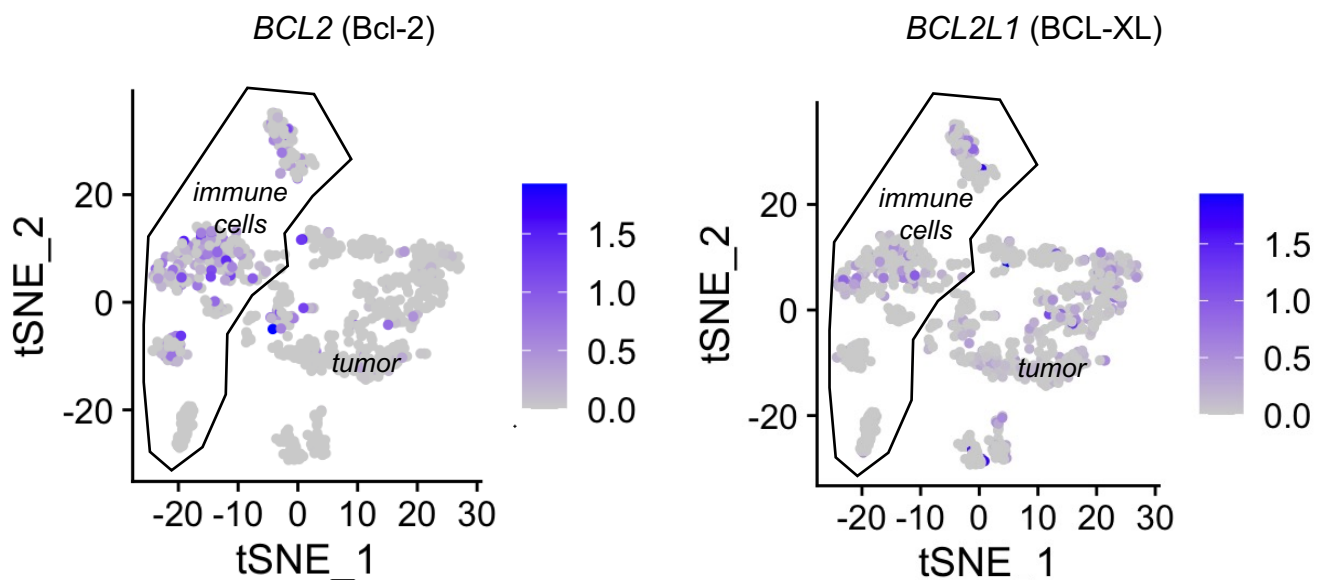
## A



## B



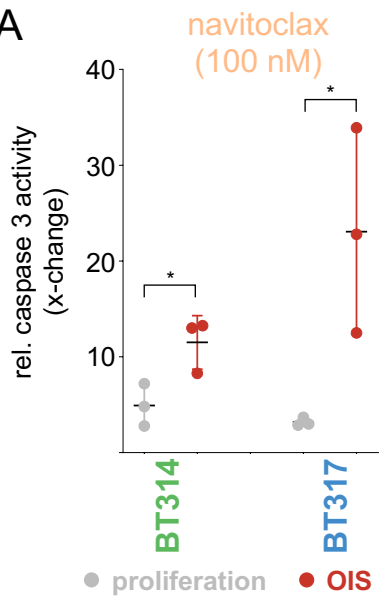
## C



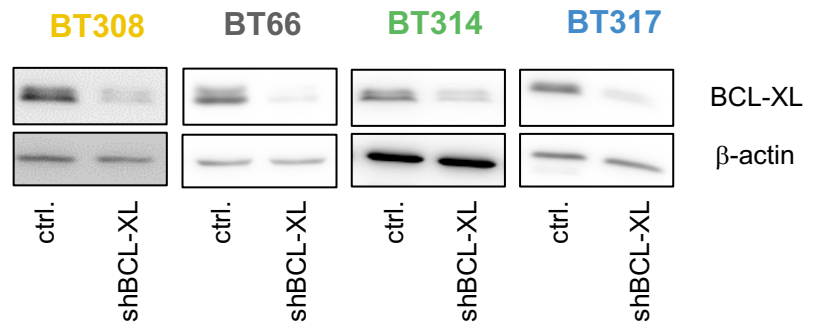
**Supplementary Figure 3: Expression of anti-apoptotic BCL-2 members in PA. A** Boxplots depicting *BCL2*, *BCL2L2* and *MCL1* mRNA expression in four PA cell lines in proliferation vs. OIS compared to normal cerebellum (n=18) and primary PA (n=191) (Tumor Pilocytic astrocytoma (DKFZ) - Kool; R2 internal identifier: ps\_mkheidel\_mkdkfz209\_u133p2). Differences between two groups were analyzed using unpaired t-test. \* p<0.05, \*\* p<0.01, \*\*\* p<0.001. **B** Western blots of BCL-2, BCL-W and MCL-1 protein expression in four PA cell lines in proliferation and OIS mode. **C** tSNE analysis of *BCL2* and *BCL2L1* mRNA expression in PA single cell RNA sequencing data. Bcl-2 is predominantly expressed in the immune cell clusters.

# Supplementary Figure 4

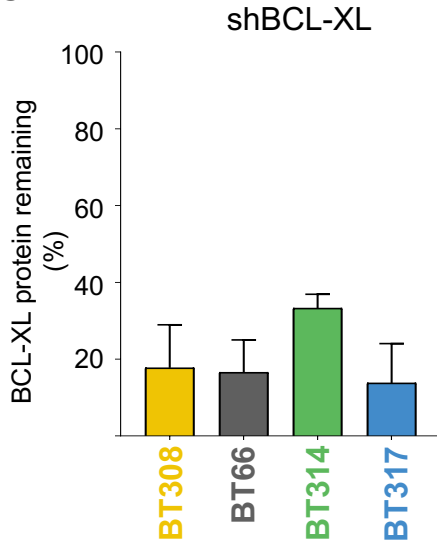
**A**



**B**



**C**

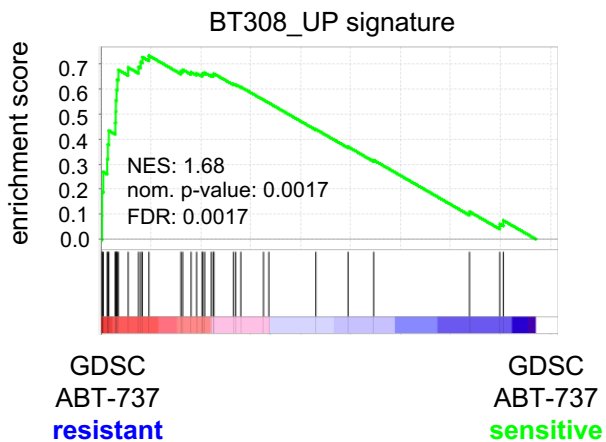


**Supplementary Figure 4: Caspase 3 activity in proliferation vs. OIS and dependence of PA cell lines on BCL-XL.** **A** Caspase 3 activity relative to DMSO control in proliferation vs. OIS after 24h treatment with 100 nM navitoclax (mean +/- SD, n=3). Unpaired t-test: \* p<0.05. **B** Representative western blots. PA cell lines in OIS were transduced with lentiviral shRNA against BCL-XL or non-silencing control shRNA (ctrl.) 96h before lysis. **C** Densitometric quantification of western-blot data. Band intensity of BCL-XL protein in BCL-XL knocked cells (96h after lentiviral infection) was measured and normalized to the intensity in cells transduced with control shRNA (n= 3 biological replicates; mean +/- SD).

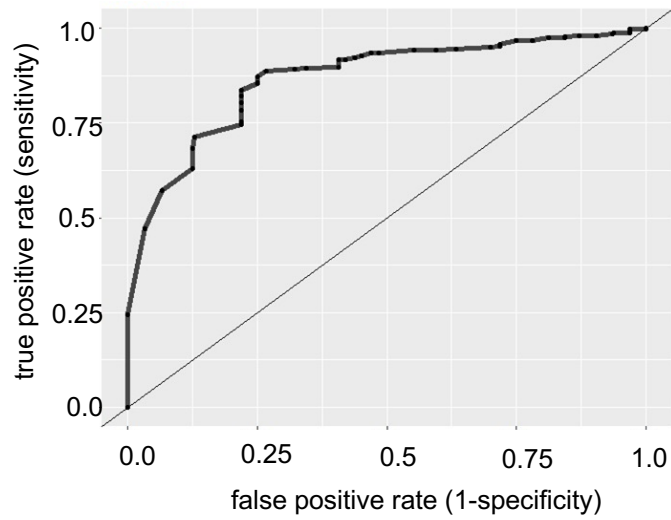


# Supplementary Figure 5

A



B



**Supplementary Figure 5: Difference in gene expression between the BCL-XLi resistant cell line DKFZ-BT308 (BT308) and the BCL-XLi sensitive cell lines DKFZ-BT66 (BT66), DKFZ-BT314 (BT314) and DKFZ-BT317 (BT317).** **A** GSEA enrichment plot depicting the comparison of BT308\_UP signature expression between the two GDSC2 cell line groups “ABT-737 resistant” ( $IC_{50}$  z-score  $>0$ ;  $n=402$ ) and “ABT-737 sensitive” ( $IC_{50}$  z-score  $<-2$ ;  $n=48$ ) **B** ROC curve of the binary logistic regression analysis of the BT308\_UP signature in 412 GDSC cell lines assigned to two groups “navitoclax resistant” and “navitoclax sensitive”.